Study on the Matrix Pencil Method with Application to Predict Time-domain Response of a Reverberation Chamber

Song Wang, Zhan C. Wu, Lei Du, Guang H. Wei, and Yao Z. Cui

Research Institute of Electrostatic and Electromagnetic Protection
Mechanical Engineering College, Shijiazhuang, 050003, China
wansonde@gmail.com

Abstract─ The full wave simulation of reverberation chamber in time domain usually takes large computational time because of its resonant characteristic. This contribution makes the pioneer exploration of accelerating this kind of simulation by time-domain signal prediction. The prediction technique is based on the well known matrix pencil method (MPM). An approximation to the existing MPM is proposed to obtain a new kind of MPM, which is more computationally efficient. To conduct the prediction effectively, the signal's oversampling should be avoided and the singular values appeared in MPM should be judged appropriately. The signal can be re-sampled according to Nyquist sampling law while the singular values can be selected by the newly proposed criterion based on cavity theory. For wideband time-domain responses, it is suggested to apply digital band-pass filter before prediction to get higher precision. Using the proposed methods, the computational time can be reduced almost 50 % for the reverberation chamber's FDTD simulation.

Index Terms – Digital band-pass filter, FDTD, matrix pencil method, reverberation chamber, and signal prediction.

I. INTRODUCTION

The reverberation chamber (RC) is an essentially electrically large cavity made of highly reflective metallic walls and excited by a source. Acting as a lower cost alternative to anechoic chambers or open area test sites, RC has become an attractive electromagnetic compatibility test facility recently [1]. It has the advantages of producing a statistically uniform field within a relatively large volume, generating high-peak fields from comparatively modest input powers, and isolating the test environment from a potentially noisy ambient environment.

Numerical modeling plays an important role in the process of RC design and analysis, and there is a variety of modeling methods as reviewed in [2]. Recently, some hybrid methods both in time-domain [3] and frequency-domain [4] have attracted much attention in the field of RC's proper simulation. To sum up, a large proportion of the correlation studies adopted the time-domain methods to take advantage of wideband analysis. The finite-difference time-domain (FDTD) method [5] is the typical one because of its explicit scheme and wide applicability. However, there exists a well known problem that it is hard to reach convergence in RC's time-domain simulation because of its strong high-Q resonances [6, 7]. Using the advanced computational techniques, such as domain decomposition and parallel computation, could alleviate this contradiction to a certain degree. But a more general solution to this problem seems to be time-domain signal prediction, i.e., using the early signal records to predict the late signal response for accurate frequency domain parameter estimation. Although the RC's numerical modeling has attracted many attentions, its accelerated simulation by this way is rare to be seen.

In time-domain simulation, a Gaussian pulse excitation is usually applied whose pulse width is much shorter than the whole simulation time. Therefore, the electric field (E-field) response within the RC is almost determined by the RC's geometry. What's more, because the excitation signal has a specific frequency range, the E-field

response could be regarded as the sum of exponentially damped sinusoids with the damping rate related to RC's losses. Therefore, it is feasible to predict the remaining response using the complex exponentials extracted from the truncated response.

The matrix pencil method (MPM) is proposed to estimate parameters of exponentially damped /undamped sinusoids in noise [8], which is more computationally efficient than the polynomial method. Several modified versions of MPM have been studied since it is firstly introduced. B. Lu proposed the improved MPM using low-rank Hankel approximation [9]. Recently, MPM has attracted many attentions [10, 11] and has contributed to solving several computational electromagnetic problems [11-13].

In this contribution, the time-domain response of RC is fitted to a model of sum of complex exponentials and a new kind of matrix pencil method is proposed based on an approximation to the existing modified matrix pencil method (MMP). Through comparison, this method is demonstrated to be more computationally efficient and to retain the same precision. Before obtaining acceptable predicting results, special attention should be paid to signal's proper sampling and singular values' appropriate judgment. Fortunately, in the case for RC's time-domain response's prediction, the required major singular values for MPM could be estimated effectively according to cavity theory. Since the computing time for prediction can be neglected compared to that of RC's numerical simulation, the proposed hybrid method combing simulation and prediction can accelerate the time-domain simulation of an RC considerably.

II. MODELING RC'S TIME-DOMAIN RESPONSE

In this section, the RC's time-domain response is analysed theoretically ending up with the linear fitting model, i.e., sum of exponentially damped complex exponentials. On the one hand, the RC's stored energy U meets,

$$\frac{dU}{dt} = P_{\mathrm{t}} - P_{\mathrm{d}} = P_{\mathrm{t}} - \frac{\omega}{Q}U \qquad (1)$$

where p_{t} is the net power delivered into RC, p_{d} is RC's total dissipated power, ω is the angular frequency, and Q is the quality factor embodying the overall losses of a real RC. The equation is

expanded using the definition of Q [14]. Solving this differential equation leads to,

$$U = U_0 \mathrm{e}^{-\frac{t}{\tau}}, t \geq 0 \qquad (2)$$

where U_0 corresponds to the stored energy when the excitation pulse is terminated and $\tau = Q/\omega$ is the time constant of RC [14]. According to the cavity theory, the amplitude of E-field strength is directly proportional to the square root of U. Moreover, the E-fields are assumed to be statistically uniform. Therefore,

$$|E_x|,|E_y| \text{ and } |E_z| \propto \sqrt{e^{-t/\tau}} = e^{-\frac{t}{2\tau}} \qquad (3)$$

where $|E_x|,|E_y|, \text{and } |E_z|$ correspond to the amplitude of E-field in the $x, y, \text{and } z$ orthogonal directions, respectively. In short, the E-fields within the RC decay exponentially.

On the other hand, there exist limited resonant frequency components for a settled RC within the investigated frequency band. To sum up, the time-domain response $s(k), k = 1, 2, ..., N$ of an RC excited by a pulse can be modeled as the sum of exponentially damped complex exponentials,

$$s(k) = \sum_{i=1}^{M} c_i z_i^k, k = 1, 2, 3 \cdots N \qquad (4)$$

where N is the signal's length, M is the number of major exponentials, $c_i, i = 1, 2, ..., M$ are fitting coefficients, and $z_i = e^{-\alpha_i + j\omega_i}, i = 1, 2, ..., M$ are complex exponentials with α_i being the damping factors and $\omega_i = 2\pi f_i$ the angular frequencies.

Once z_i and M are determined from the truncated early response of an RC, then $c_i, i = 1, 2, ..., M$ can be derived by solving a least-squares problem [8]. Consequently, the late response can be predicted by increasing N to be large enough.

III. DERIVATION OF A NEW KIND OF MPM

In this section, a new kind of MPM is proposed based on an approximation to the existing modified MPM.

A. Recalling the conventional MPM

The observed data (probably contaminated by noise $n(k)$) is expressed as,

$$y(k) = s(k) + n(k), k = 1, 2, ..., N . \qquad (5)$$

In order to extract $z_i, i = 1, 2, ..., M$ from $y(k)$, the Hankel data matrix Y is constructed as,

$$Y = [y_1, y_2, \cdots, y_{L+1}] \qquad (6)$$

where $\beta \square L/N$ is called pencil rate parameter satisfying $M < L < N - M$ and the column vector,

$$y_l = [y(l), y(l+1), \cdots, y(N-L+l-1)]^T \qquad (7)$$

where the superscript T denotes the transpose operator. The matrices Y_1 and Y_2 (with the same size) are obtained by removing the last and first column of Y, respectively.

The matrix pencil for Y_1 and Y_2 is defined as $Y_2 - \lambda Y_1$, with λ a complex parameter. If $n(k)=0, k=1,2,...,N$, $Y_2 - \lambda Y_1$ can be rewritten as,

$$Y_2 - \lambda Y_1 = Z_1 C [Z_0 - \lambda I] Z_2 \qquad (8)$$

where

$$Z_1 = \begin{bmatrix} z_1 & z_2 & \cdots & z_M \\ z_1^2 & z_2^2 & \cdots & z_M^2 \\ \vdots & & \ddots & \vdots \\ z_1^{N-L} & z_2^{N-L} & \cdots & z_M^{N-L} \end{bmatrix}, \qquad (9)$$

$$Z_2 = \begin{bmatrix} 1 & z_1 & \cdots & z_1^{L-1} \\ 1 & z_2 & \cdots & z_2^{L-1} \\ \vdots & & \ddots & \vdots \\ 1 & z_M & \cdots & z_M^{L-1} \end{bmatrix}, \qquad (10)$$

$$Z_0 = \mathrm{diag}\{z_1, z_2, ..., z_M\}, \qquad (11)$$

$$C = \mathrm{diag}\{c_1, c_2, ..., c_M\}. \qquad (12)$$

Because $\lambda = z_i$ is the rank-reducing number of this matrix pencil, the eigenvalues of $Y_1^+ Y_2$ can be regarded as $z_i, i = 1, 2, ..., M$, where + denotes the Moore-Penrose pseudo inverse operator. If $y(k)$ is contaminated by noises, the rank of $Y_2 - \lambda Y_1$ is probably larger than M, and the low-rank approximation to Y is proposed to suppress the noises before adopting the same procedure to derive $z_i, i = 1, 2, ..., M$ [15]. In the first step, the SVD of Y is carried out,

$$Y = U \begin{bmatrix} \Sigma & O \\ O & O \end{bmatrix} V^H \qquad (13)$$

where the superscript H denotes the conjugate transpose, U and V are made up of the eigenvectors of YY^H and $Y^H Y$, respectively and $\Sigma = \mathrm{diag}(\sigma_1, \sigma_2, \cdots, \sigma_q)$ is composed of the nonzero singular values σ_i arranged in a descending sequence. In the second step, M major singular values are selected to make up,

$$\Sigma' = \mathrm{diag}(\sigma_1, \sigma_2, \cdots, \sigma_M), M < \min(N-L, L). \quad (14)$$

Then the reduced-rank approximation (its operator $\mathcal{L}$) of Y is derived as,

$$Y' = \mathcal{L}(Y) = U' \Sigma' V'^H \qquad (15)$$

where U' and V' are obtained by choosing the front M columns of U and V, respectively. It is proved that among all the matrices with the same size of Y, Y' is the one, which has the minimum Frobenius norm deviation to Y, and this deviation decreases as M increases [11].

The simple criterion to determine M would be checking whether,

$$\sigma_M / \sigma_1 <= 10^{-p} \qquad (16)$$

where p is an appropriately chosen value according to the specific predicting data. These selected singular values can be regarded as the weight coefficients corresponding to the major resonant components. In contrast, those discarded ones having trivial values corresponds to the noisy components.

The same method as used in the noiseless case could be utilized to get z_i from Y', while an equivalent but more computationally efficient technique is to calculate the front M eigenvalues of,

$$\{V_1'^H\}^+ V_2'^H \qquad (17)$$

directly to estimate z_i [15], where (in Matlab notation),

$$V_1' = V'(1:L,:), V_2' = V'(2:L+1,:).$$

The computation burden can be alleviated in this way because the operation to obtain Y' is avoided. This conventional method is named *mp*.

B. Derivation of the new kind of MPM

While $\mathcal{L}(Y)$ does not remain the Hankel structure, the reduced-rank Hankel approximation (its operator J) is introduced to derive $J(Y)$, which possesses both the Hankel structure and rank-deficient properties. This modification is helpful in suppressing noises. By the aid of $\mathcal{H}$ known as the Hankel approximation operator. An iterative algorithm of J is available where each iteration executes $\mathcal{H}$ and $\mathcal{L}$, successively. For a given matrix X, the iterative algorithm of J is

$$J(X) = (\mathcal{H}\mathcal{L})^\infty(X) = \lim_{G \to \infty} \underbrace{(\mathcal{H}\mathcal{L} \cdots (\mathcal{H}\mathcal{L}(X)) \cdots)}_{G}. \quad (18)$$

For more details about J, the reader can refer to [16]. The modified MPM using J is stated as below, which is named *mmp1*.

1. $\tilde{Y} = J(Y)$,

2. $\tilde{Y}_1 = \tilde{Y}(:,1:L), \tilde{Y}_2 = \tilde{Y}(:,2:L+1)$,

3. $\hat{Y}_i = \mathcal{L}(\tilde{Y}_i), i = 1,2$,

4. Calculating the front M eigenvalues of $\{\hat{Y}_1\}^+\hat{Y}_2$.

The main difference from mp occurred in step 1, i.e., the pre-treatment of the original master matrix Y, which retains the Hankel structure in the process of filtering noise represented by operator $\mathcal{L}$. The subsequent steps resemble that of mp. Analyzing the computational burden of $mmp1$, $\mathcal{L}$ is the key factor because it is more time-consuming than $\mathcal{H}$ considering the SVD. In order to avoid $\mathcal{L}$, the approximation to step 3 is proposed to reduce the executions of $\mathcal{L}$ from two times to one time. That is

$$\hat{Y} = \mathcal{L}(\tilde{Y}), \hat{Y}_1 = \hat{Y}(:,1:L), \hat{Y}_2 = \hat{Y}(:,2:L+1), \quad (19)$$

in the case when $L\varepsilon 1$.

What is more, recalling the equivalent procedure mentioned above equation (17), it is preferred to derive the required M eigenvalues from matrix $\tilde{V}$ directly, rather than rely on matrix $\hat{Y}$ needing additional multiply operation between matrixes. To sum up, a new kind of MPM, named $mmp2$, is proposed as below,

1. $\tilde{Y} = J(Y)$,

2. obtain $\tilde{V}$ from $\mathcal{L}(\tilde{Y})$,

3. $\tilde{V}_1 = \tilde{V}(1:L,:), \tilde{V}_2 = \tilde{V}(2:L+1,:)$,

4. Calculating the front M eigenvalues of $\{\tilde{V}_1^H\}^+\tilde{V}_2^H$.

Because the condition $L\varepsilon 1$ is usually satisfied, the method $mmp2$ is assumed to get the almost identical results with $mmp1$ with less computation burden.

C. Validation of the proposed method

The advantage of $mmp1$ had been shown in [9] compared to mp. As $mmp2$ is proposed based on $mmp1$, its feasibility and effectiveness is validated by comparing the simulation result from $mmp1$ and $mmp2$. The similar example as in [16] is employed. $M = 10$, $N = 1000$, and $\beta = 0.60$. The symbol $\alpha_i, i = 1,2,...M$ are randomly chosen from $1.0/N$ to $1.5/N$. In Matlab notation, this is

$$\alpha = \frac{1}{N} + \text{rand}(1,M) * \frac{1}{2N}.$$

Similarly, c_i are randomly chosen within [1, 2], and ω_i within [0.35*2π, 0.5*2π]. Once these parameters are determined, series $s(k)$ are built according to equation (4).

As we focus on the real-time signal prediction for RC's response, only the real parts of $s(k)$ are considered. Both the methods $mmp1$ and $mmp2$ are used to extract z_i under different signal-to-noise ratio (SNR), which is defined as

$$\text{SNR} = 10 \times \log 10 \left(\frac{\text{var}(s)}{\text{var}(n)} \right). \quad (20)$$

Then, c_i are derived using the least-square method. Because the complex exponentials are used to fit the real-time series, setting the number of the selected major singular values to be 20 is optimal meaning 10 pairs of conjugate complex exponentials. The original and fitted signals are named y_o and y_s, respectively. The prediction is achieved through lengthening y_s by enlarging N. Here, both y_o and y_s are lengthened to 2000. That is to say only 1000 data are used to determine the unknown parameters, such as z_i and c_i. The second half signal is obtained through prediction. Their relative error

$$\varepsilon = \frac{\| y_s - y_o \|_2}{\| y_o \|_2}, \quad (21)$$

is regarded as the indicator for evaluating the performance of the two methods. As shown in Fig. 1, ε is exactly the same for both methods and it decreases as the SNR increases. This coincidence demonstrates the effectiveness of the approximation presented by equation (19). In fact, ε is a severe indicator, because the agreement is already quite acceptable when ε is below 0.15. In detail, the fitting and predicting performance under $\varepsilon = 0.10$ are shown in Fig. 2 and 3. As we can see, satisfactory agreement is reached.

What is more, the consumed time t_1 and t_2 of $mmp1$ and $mmp2$, respectively, on a PC with a 3.0 GHz CPU is compared in Table I. Obviously, the proposed method $mmp2$ is more computationally efficient than $mmp1$ with the same precision. This is because J can reach convergence within several iterations and $mmp2$ reduces the operation time of $\mathcal{L}$ effectively. Besides, the computation time increases as the SNR decreases, because lower SNRs usually correspond to more iterations in J.
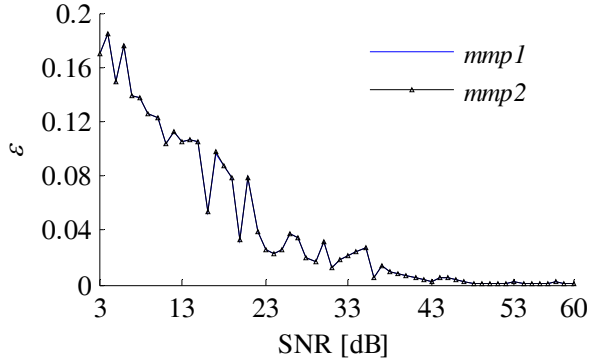
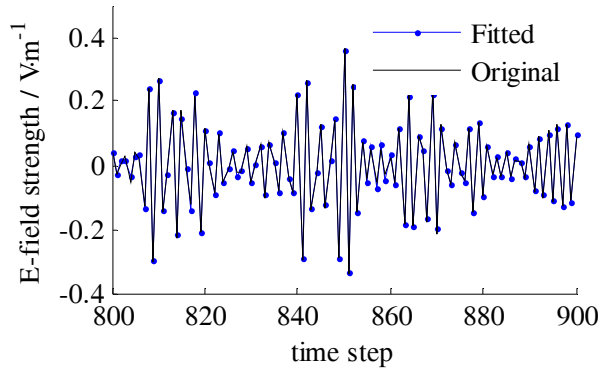Fig. 1. ε from *mmp1* and *mmp2* versus SNR.
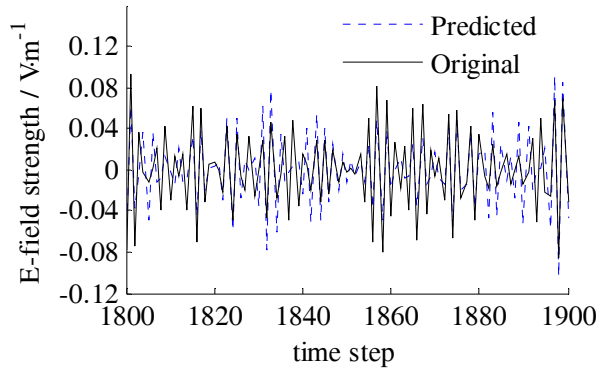

Fig. 2. Local performance of fitting.

Fig. 3. Local performance of predicting.

Table. I. Comparison of t_1 (*mmp1*) and t_2 (*mmp2*).

SNR	t_1 / s	t_2 / s
5 dB	17.4	13.6
10dB	14.7	11.8
15dB	10.5	8.9
25dB	7.9	6.2
40dB	6.4	5.3

IV. APPLICATION TO ACCELERATING RC'S FDTD SIMULATION

Through predicting the RC's time-domain response from the truncated simulated signal, the RC's simulation is accelerated. Here, we focus on RC's FDTD simulation, but the prediction methodology is also applicable to the results from other time-domain simulation methods.

A. Configurations

The investigated RC's dimension is 10.5 m × 8.0 m × 4.3 m with the lowest usable frequency about 80 MHz. It is equipped with two different stirrers rotating in step-by-step mode, i.e., mechanical stirring. With the aid of the published codes in [5], it is simulated by FDTD with the spatial meshing step $dx = dy = dz = 0.1$ m and time step $dt = 1.73 \times 10^{-10}$s. The transmitting antenna is a 1.6 m long dipole antenna modeled using the thin-wire technique [5]. A modulated Gaussian pulse with the specified frequency band (80~120) MHz is applied to the antenna.

On the disposal of RC's losses, treating the conductivity of the materials in numerical model as the real values is found to generate much higher electric field strength than measurement data [7] because the real RC includes many kinds of losses and they can hardly be reproduced by RC's numerical model. Alternatively, drawing on the proposition from [7], the approximation method is introduced by regarding the material of the RC as PEC and setting the air's conductivity σ_{air} to be about $1.5\times10^{-5}\sim2\times10^{-5}$ S/m [17]. That is to say the overall losses of the RC approximately equals to the losses on the RC's inner air volume. This value is higher than 10^{-5} S/m in [7] because our RC's material is mainly galvanized steel rather than aluminum and its reflection coefficient is lower than aluminum [17]. It is worth noting that we emphasize on the prediction on the time-domain response rather than the details about RC's numerical modeling.

The simulation runs for a number of time steps N_{ts} until the amplitude of the E-field strength is attenuated to nearly 1 % of the peak value. Eight sampling points within the RC's working volume are selected for E-field output at x, y, and z directions. The proposed method *mmp2* is adopted for the prediction.

B. Implementation issues

The RC's time-domain response from FDTD simulation is believed to possess a relatively high SNR. Acceptable agreement can be reached between the predicted response and the simulated signal for RC providing both the following issues are taken into accounts, i.e., signal re-sampling and appropriate choice of M (the number of the major singular values).

The signal re-sampling refers to ensuring the signal is sampled appropriately before prediction according to the Nyquist sampling law. Under this configuration, as the sampled frequency $1/dt$ is much higher than the ceiling of the investigated frequency band, these E-field signals are re-sampled at $1/20$ times $1/dt$ with the Nyquist sampling law still satisfied. In fact, the re-sampling is crucial for good prediction results because oversampling means redundancy and additional computation burden for MMP.

Besides the signal's re-sampling, the key parameter M can no longer be determined as effortless as in section III. The simulation data show that determining M by the criterion represented in equation (16) is neither reliable nor convenient because controlling the key parameter p calls for trial and error attempts. Alternatively, since M depends on the number of resonant frequencies, it can be determined according to the number of the RC's activated resonant modes within the simulated frequency band. We manage to estimate the total number of activated resonant modes approximately based on the cavity theory. In this way, the resonant frequency (in Hz) corresponding to a potential resonant mode can be expressed as,

$$f_{m,n,p} = \frac{c}{2}\sqrt{\left(\frac{m}{L_{RC}}\right)^2 + \left(\frac{n}{W_{RC}}\right)^2 + \left(\frac{p}{H_{RC}}\right)^2} \quad (22)$$

where c is the velocity of light in vacuum and L_{RC}, W_{RC}, H_{RC} are the rectangular cavity's length, width, and height, respectively. Using equation (22), about 90 different resonant frequency components are determined for our simulating frequency band. So it is reasonable to set $M = 180$. Although, the RC equipped with some stirrers usually demonstrates more complex field distribution with a relatively larger density of resonant modes compared with the empty case, the prediction results show that it is indeed an effective approach to derive M for MPM. This can

be understood considering that the number of 'activated' resonant modes in the RC with stirrers is close to that of the 'potential' resonant modes in the same RC without stirrers.

C. Results of prediction

We took two cases for results' checking. In case one, we assume an RC with the same dimensions is under low losses and set $\sigma_{air} = 1 \times 10^{-5}$ S/m. The required N_{ts} is 40000 corresponding to about 70 minutes' operation on a PC with a 3.0 GHz CPU. Each of the obtained E-fields' responses is projected to 2000 data by the re-sampling method. Similarly, the first half data are used by *mmp2* to determine the unknown parameters and the relative error ε_t with the same definition is used for performance checking.

According to equation (14), the span of the key parameter β should satisfy,

$$\min\{\beta N, (1-\beta)N\} > M . \quad (23)$$

Through simulation optimization, the smallest ε is obtained for most sets of the E-field signals when $\beta = 0.6$. Its results are shown in Fig. 4. The fitted and predicted signal converges to zero as the same as the original simulated signal. From local checking, acceptable agreement is obtained.

Moreover, the fitting-predicting performances for all these sets of E-field signals from different locations within the working volume of the RC are shown in Fig. 5 where the 10th set corresponds to the results in Fig. 4. Acceptable performance is obtained with all ε_t below 15 %. The results are close to each other since all these 24 sets of sampled signals share the same RC's resonant characteristics.

In essence, only the second half signal by prediction is of significance. So additional attention is paid to the semi-simulated semi-predicted signal whose relative error between the complete simulated data is ε_{tc}, which is certainly smaller than ε_t as shown in Fig. 5. Although the improvement degree from ε_t to ε_{tc} is far less than 50 %, which means the prediction is not as good as the fitting, the indispensable effect of prediction can be seen in Fig. 6. Here, the relative error in frequency-domain between the complete 2000 simulated data (after re-sampling) and the front 1000 truncated data (truncation means the rest of signal data are assigned to zeros) is denoted as ε_f, while the relative error between complete signal and semi-simulation semi-prediction signal is

labelled ε_{fc}. From Fig. 6, ε_{fc} is indeed smaller than ε_f, so the method combining simulation and prediction is feasible and effective.
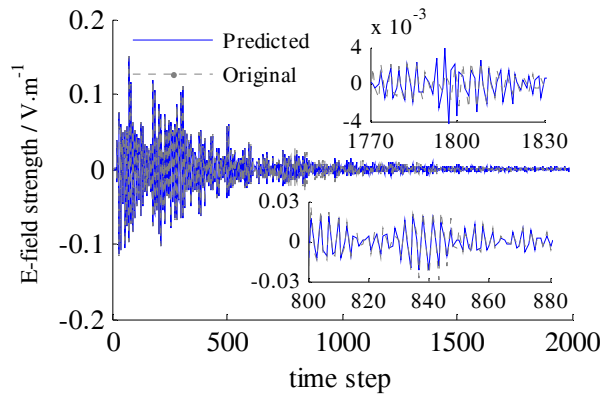

Fig. 4. Performance of fitting and predicting for RC's time-domain response.
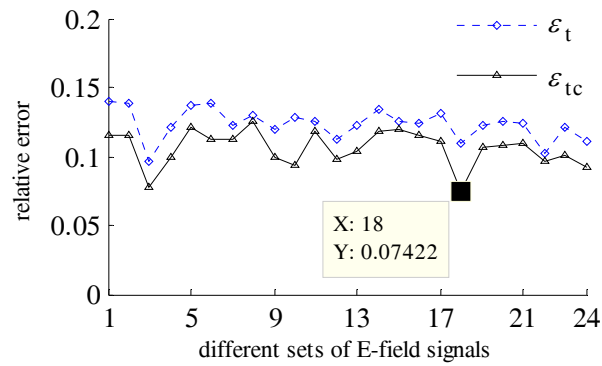

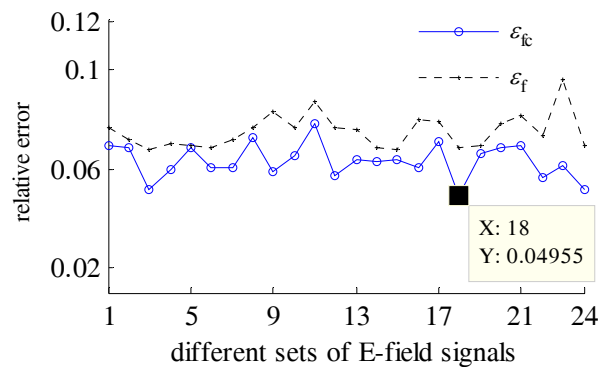Fig. 5. Performance versus different sets of E-field signals.

Fig. 6. Comparison of relative Error in frequency-domain.

In case two, since it had been validated that the overall losses of our RC in reality can be approximated by increasing σ_{air} to about 2.0×10^{-5} S/m [17], we took $\sigma_{air} = 2.0 \times 10^{-5}$ S/m with $N_{ts} = 26000$, which means the higher level of losses the fewer of simulation time steps. Using the same method for signal re-sampling, the length of the usable data shrunk to 1300. Similarly, the first half is used to predict the second half employing method *mmp2*, where M is also set to 180. The prediction performances are showed by the dashed line in Fig. 7, which are a little worse than that in Fig. 5. The relative error ε_{tc} for some set of the E-field signals even exceeds 30 %. The main reason is that the length of available data used in *mmp2* shrunk a lot compared with that in case one. Consequently, the formerly optimized parameter $\beta = 0.6$ is no longer the preferential choice for case two. After optimization, setting $\beta = 0.7$ can obtain quite acceptable results for all sets of the E-field signals as shown in Fig. 7.
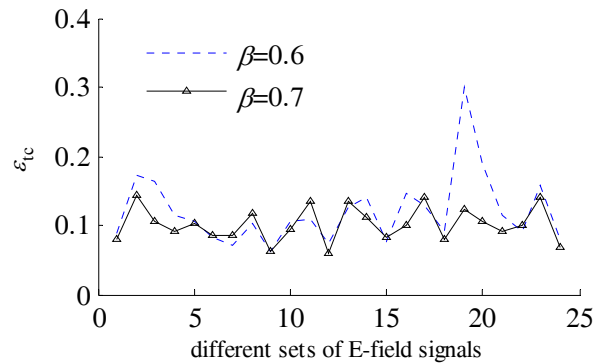

Fig. 7. Comparison of ε_{tc} with different β.

In other cases, when the investigated frequency band is enlarged, it is not easy to ensure ε_{tc} below 15 %. That is because the number of potential resonant modes will increase swiftly as the frequency band expands. From our preliminary exploration, in order to obtain acceptable prediction results, the number of properly sampled data used for prediction should be several times of the total number of resonant components. Therefore, in order to get higher precision, it is suggested to apply digital band-pass filter to the wideband time-domain responses before prediction.

V. CONCLUSION

In this contribution, accelerating RC's time-domain simulation employing signal's prediction is shown to be feasible. Since the RC's time-domain response has the characteristics of resonance and exponentially damping trend, it can be formulated as a sum of complex exponentials whose unknown parameters can be estimated effectively by the matrix pencil method. An approximation is proposed to save unnecessary reduced-rank decomposition in the MPM, which leads to a new kind of MMP, which is more computationally efficient and retains the same precision. In its application to RC's time-domain response prediction, the major singular values can be estimated appropriately by the newly proposed criterion base on the cavity theory. Simulation data show that the RC's time-domain response from FDTD modeling can be fitted and predicted effectively. Noting that the consumed computing time by MMP can be neglected compared with that by FDTD simulation, the hybrid method combining simulation and prediction can save considerable time for RC's time-domain simulation (almost 50%). Moreover, the employment of this predicting technique is independent of the RC's simulation tool. It can give reasonable results only if the under-predicting signal has an appropriate sampling rate and the major singular values are selected effectively.

REFERENCES

[1] J. H. Rudander, I.-E.-Khuda, P.-S. Kildal, and C. Orlenius, "Measurements of RFID tag sensitivity in reverberation chamber," *IEEE Antennas And Wireless Propagation Letters*, vol. 10, no. 1, pp. 1345-1348, 2011.

[2] C. Bruns and R. Vahldieck, "A closer look at reverberation chambers 3-D simulation and experimental verification," *IEEE Transactions on Electromagnetic Compatibility*, vol. 47, no. 3, pp. 612-626, 2005.

[3] S. Lallechere, P. Bonnet, S. Girard, F. Diouf, and F. Paladian, "Evaluation of FVTD dissipation and time-domain hybridization for MSRC studies," *Presented at the 23rd Annual Review of Progress in Applied Computational Electromagnetics*, Verona, Italy, 2007.

[4] H. P. Zhao and Z. X. Shen, "Efficient modeling of three-dimensional reverberation chambers using hybrid discrete singular convolution-method of moments," *IEEE Transactions on Antennas and Propagation*, vol. 59, no. 8, pp. 2943-2953, 2011.

[5] A. Z. Elsherbeni and V. Demir, *The Finite-Difference Time-Domain Method for Electromagnetics with MATLAB Simulations*, SciTech Publishing Inc., Raleigh, NC, 2009.

[6] H. Bruns, C. Schuster, and H. Singer, "Numerical electromagnetic field analysis for EMC problems," *IEEE Transactions on Electromagnetic Compatibility*, vol. 49, no. 2, pp. 253-262, 2007.

[7] F. Moglie, "Convergence of the reverberation chambers to the equilibrium analyzed with the finite-difference time-domain algorithm," *IEEE Transactions on Electromagnetic Compatibility*, vol. 46, no. 3, pp. 469-476, 2004.

[8] Y. Hua and T. K. Sarkar, "Matrix pencil method for estimating parameters of exponentially damped/umdamped sinusoids in noise," *IEEE Transactions on Acoustics, Speech and Signal Processing*, vol. 38, no. 5, pp. 814-824, 1990.

[9] B. Lu, D. Wei, B. Evans, and A. Bovik, "Improved matrix pencil methods," *presented at the Conference Record of the Thirty-Second Asilomar Conference on Signals, Systems & Computers*, 1998.

[10] K. Chahine, V. Baltazart, and Y. Wang, "Parameter estimation of damped power-law phase signals via a recursive and alternately projected matrix pencil method," *IEEE Transactions on Antennas and Propagation*, vol. 59, no. 4, pp. 1207-1216, 2011.

[11] Y. Liu, Z. Nie, and Q. Liu, "Reducing the number of elements in a linear antenna array by the matrix pencil method," *IEEE Transactions on Antennas and Propagation*, vol. 56, no. 9, pp. 2955-2962, 2008.

[12] J. Ritter and F. Amdt, "Efficient FDTD/matrix-pencil method for the full-wave scattering parameter analysis of waveguiding structures," *IEEE Transactions on Microwave Theory and Techniques*, vol. 44, no. 12, pp. 2450-2456, 1996.

[13] Y. Yang, S. Hu, R. Chen, H. Zhang, and T. Liu, "FDTD analysis with modified matrix pencil method for the UC-EBG lowpass filters," *Microwave and Optical Technology Letters*, vol. 44, no. 1, pp. 37-41, 2005.

[14] IEC 61000-4-21, *Electromagnetic Compatibility (EMC) - Part 4-21: Testing and Measurement Techniques - Reverberation Chamber Test Methods*, ed: International Electrotechnical Commission (IEC), pp. 40-44, 2011.

[15] T. Sarkar and O. Pereira, "Using the matrix pencil method to estimate the parameters of a sum of complex exponentials," *IEEE Antennas and Propagation Magazine*, vol. 37, no. 1, pp. 48-55, 1995.

[16] Y. Li, K. R. Liu, and J. Razavilar, "A parameter estimation scheme for damped sinusoidal signals based on low-rank Hankel approximation," *IEEE*

Trans. on Signal Processing, vol. 45, no. 2, pp. 481-486, 1997.

[17] S. Wang, Z. Wu, G. Wei, Y. Cui, and L. Fan, "A new method of estimating reverberation chamber Q-factor with experimental validation," *Progress In Electromagnetic Research Letters*, vol. 36, pp. 103-112, 2013.

Song Wang was born in 1987, Hebei province, China. He received the B.Sc. degree from Beihang university, Beijing, China, in 2010, and the M.Eng. degree from Institute of Electrostatic and Electromagnetic Protection, Mechanical Engineering College, Shijiazhuang, China. He is currently working towards the Ph.D. degree and his research interests include computational electromagnetic and electromagnetic tests in reverberation chamber.